Fusion cross-sections using different nuclear proximity potentials and radii at low energy

A dissertation submitted

For partial fulfillment of the requirement for

The award of the degree of

Master of Science

in

Physics

(2018-2019)

Under the guidance of

Dr. Raj Kumar

(Assistant Professor)

Submitted by

Manpreet Kaur Puar

(301704018)

SCHOOL OF PHYSICS AND MATERIALS SCIENCE

THAPAR INSTITUTE OF ENGINEERING AND TECHNOLOGY,

PATIALA – 147004, (Punjab) INDIA

CERTIFICATE

This is to certify that this thesis entitled "**Fusion cross-sections using different nuclear proximity potentials and radii at low energy"** is submitted by **Ms. Manpreet Kaur Puar** (Roll. No. 301704018) in the fulfilment of the partial requirement for the award of degree of Master in Science in Physics from School of physics and Material Science, Thapar Institute of engineering and technology, Patiala (Punjab), India. It is an exclusive record of candidate's own research under the supervision of Dr. Raj Kumar. This Thesis in part or full has not been submitted in any other institute for award of such kind of degree.

Manpreet

Date: (Manpreet Kaur Puar)

Raj Kumar

Dr. Raj Kumar

(Assistant Professor)

School of Physics and Materials Science

Thapar Institute of engineering and technology,

Patiala-147004

ACKNOWLEDGMENT

I am submitting my Thesis for the fulfilment of my 'M.Sc.' degree. This work would not have been accomplished without the help, support and guidance. I express my deep gratitude and respect to my supervisor **Dr. Raj Kumar** (Assistant Professor, School of Physics and Materials Science) for his strong motivation, trust and constant encouragement during the course of work. I thank him for his great patience, constructive criticism and for giving me the opportunity to undertake this project. The meaning of my life and work is incomplete without paying regards to my respected family whose blessings and continuous encouragement have shown me the path to achieve my goals.

My special thanks to **Ms. Shivani Jain**, research scholar for their moral support, friendship, patience, love and kindness to finish this work. Although having a hectic timetable she was there when I looked-for her. I am very glad that she helped me throughout the thesis patiently. I am also thankful to **Ms. Navjot Kaur Virk**, research scholar, for helping me and the research scholar of nuclear physics lab for their help when I needed.

I own my sincere gratitude towards my family for their support and love that gave me power and strength to complete this dissertation work successfully. I am also grateful to my friend Shivangi Bhatia for her help and support during the course of this work.

Manpreet

Manpreet Kaur Puar

ABSTRACT

Fusion cross-sections using different nuclear proximity potentials and radii at low energy have been studied for ^{16}O, ^{40}Ca and ^{48}Ca-induced reactions. The variations in the barrier height of interaction potential calculated by using nuclear proximity potential of Blocki et. al. (Prox77) proximity potential has been observed by using nuclear radii of Prox00 and Denisov DP within the Prox77. The respective changes in the fusion barrier heights have been further analyzed in terms of fusion cross-sections using Wong formula. The theoretically calculated fusion cross-sections for ^{16}O, ^{40}Ca and ^{48}Ca-induced reactions are compared with the corresponding experimental data.

The present work consists of three chapters.

CHAPTER 1

Chapter 1 contains the general introduction to nuclear physics, nuclear reaction (such as nuclear fusion and fission) and their properties. In this dissertation, the whole work is concentrated to study or explore the behavior of nuclear fusion reactions occurred by heavy-ion collisions at the low energy region (< 15 MeV/nucleon). As it is known that, the ion-ion potential is very important tool to elaborate the behavior of nuclear fusion interaction across the Coulomb barrier energies. Also, the interaction potential gets influenced with the effect of different choices of nuclear radii. In view of this, the role of different nuclear radii used within Proximity 1977 potential have been analyzed by calculating fusion cross-sections.

In this chapter, we have considered only spherical choices of colliding nuclei.

CHAPTER 2

Chapter 2 consists of methodology of different proximity potentials like Prox77, Prox00 and Denisov DP. The nuclear part of the total interaction potential is calculated using above mentioned proximity potentials, and corresponding variations have been observed in the barrier height (V_B) and barrier position (R_B) of the total interaction potential. Further, V_B and R_B as input are used within the Wong formula to calculate the fusion cross-sections. The theoretically estimated cross-sections are compared with the available experimental data.

A broad description regarding above given potentials and Wong formula are illustrated in chapter 2.

CHAPTER 3

Chapter 3 is based on the outcomes and discussion regarding the behavior of total interaction potentials and corresponding fusion cross-sections with the effect of different nuclear radii taken from Prox77, Prox00 and Denisov DP potentials. The analysis is exercised for the formation of Zr^{*} and Nd^{*} isotopes from ^{16}O, ^{40}Ca and ^{48}Ca – induced reactions.

Table of Contents

Chapter 3

List of figures

Chapter 1:

Chapter 3:

List of Tables

Chapter 3:

Chapter 1

Literature Review

Chapter 1

Introduction:

1.1 General:

The Universe is fabricated of countless stars, planets and many more undiscoverable things, which inspired the scientists and scholars of all time to give enormous contributions in understanding its perplexing nature. At the initial stages of investigations, the awareness about the beginning of Universe was not appropriate and sufficient. To demonstrate the origin of Universe with a time interval, the scientists have given a great theory, called Big Bang theory, which presents a comprehensive knowledge regarding the natural events. The expansion of Universe from a very high-dense and energetic state shows so many physical processes. The ideas behind these events are more expressible via a detailed description of the subatomic world. The electrons orbiting around a highly-dense nucleus within a very small region of size about 10^{-10}m, this region is called as atom, defines the behavior of subatomic world. The existence of an atom is possible due to the interaction between the nucleus, which is comprised of positively charged protons and neutral neutrons, and electrons. The interactions between the constituents of atom are developed on the basis of fundamental interactions i.e. electromagnetic force, strong (nuclear) force and weak force. In other words, the interactions between the subatomic particles illustrate the natural phenomena at a very small or discrete level, which cannot be measured by a direct process. Till date, the study of atom given by the scientists is well established and adequate enough to describe the physical processes at the atomic scale. However, the behavior of a bare nucleus is still uncertain, due to unpredictable nature of nucleons (protons and neutrons) residing inside it. Thus, the field of Physics in which the interactions between the nucleons and nuclei have been studied is named as Nuclear Physics, encircling from subatomic to the cosmic world.

Exploration of nuclear properties is a progressive, effective and dynamic field of analysis. With a better understanding and intense study over the atomic nucleus and its constituents, it has been known that the nucleons inside the nucleus are bound to each other because of an attractive short-range strong nuclear force. In

addition of this force, there is another force due to the positively charged protons, which is named as long-range repulsive Coulomb force. Unlike Coulomb interactions between the protons, the knowledge of strong or nuclear force is not well established. The investigation on the behavior of this force for nuclei belonging to different mass-region of periodic table is still under progress. In view of this, so many people are giving various theories and models to probe the static and dynamic nature of the nucleus [1-5]. The exploration of matter, in view of the interaction between nucleons/nuclei, leads us to give a better perception towards the effects at both the microscopic and macroscopic levels.

1.2 Nuclear reactions:

In Nuclear Physics, the nuclear reaction is considered as an essential aspect to comprehend the interaction between the two nuclei, which further causes a conversion of one nuclide to another. The interaction between cosmic rays and matter is an example of natural nuclear reaction. Enormous efforts by the scientists have led to employ artificial nuclear reactions in order to obtain the nuclear energy as per requirement. Till date, the possible number of nuclear reactions occurred in the whole universe is immense. But, there are lots of notable nuclear reactions, like elastic/inelastic scatterings, direct reactions, spontaneous decay, heavy-ion reactions which generally involve nuclear fusion and fission reactions (shown in Fig. 1.1 and 1.2), etc. In this dissertation, the whole work is concentrated to study or explore the behavior of heavy-ion nuclear fusion reactions, which are induced by the nucleus with mass greater than the alpha nucleus (^{4}He). In heavy-ion reactions, the variety of nuclear collisions can be exemplified in terms of range of energies given to the incident beam/projectile. When the energy of beam particles in a nuclear reaction is below 15MeV/nucleon, it caters the low energy reactions, the energy within the range of 15 and 500MeV/nucleon corresponds to intermediate energy reactions, and finally the projectile energy above 500MeV/nucleon accounts for high energy reactions. Henceforth, these different ranges of energy show a vast regime of nuclear physics to study the heavy-ion reactions at different aspects.

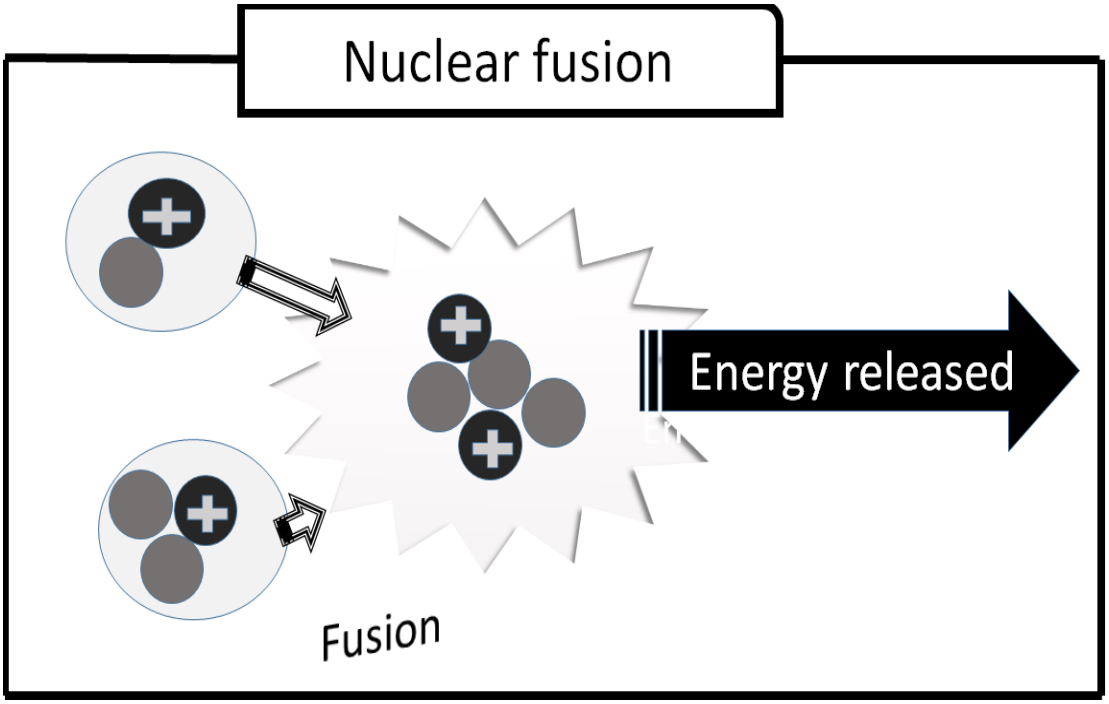

Fig. 1.1 A schematic diagram of nuclear fusion process.

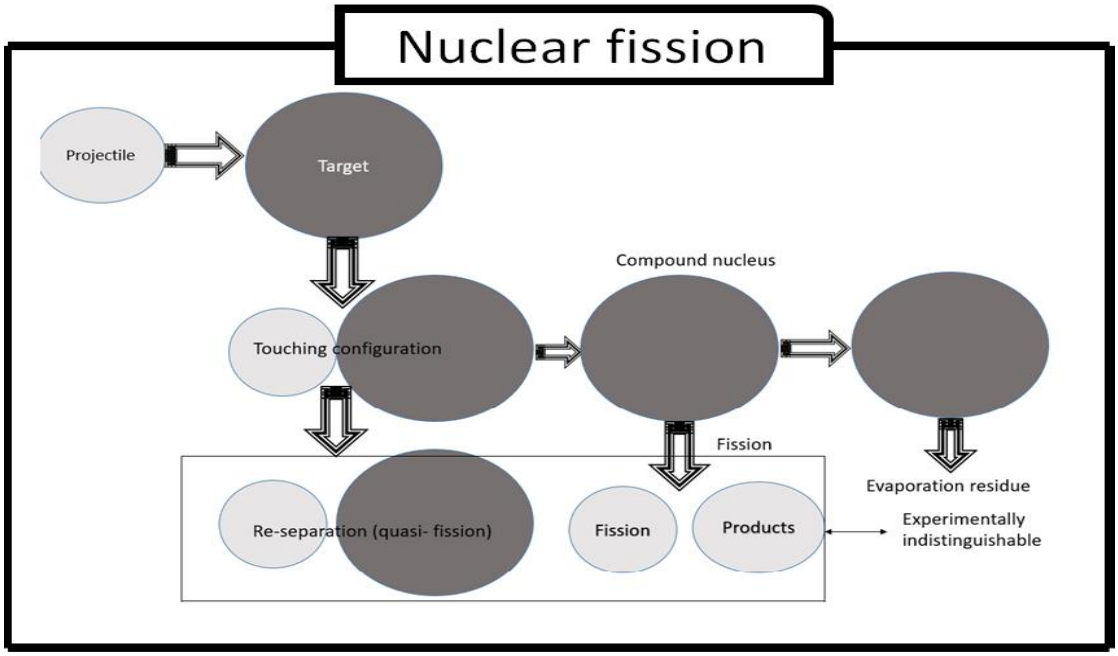

Fig. 1.2 A schematic diagram of nuclear fission process.

1.3 Nuclear fusion reactions:

In nuclear fusion reactions, the projectile acquired with some external energy knocks the surface of target to fuse, and subsequently form a new heavy nucleus, which is called Compound Nucleus (CN). The formation of CN is possible when the values of angular momenta introduced via the entrance channel are smaller than that of the composite system. In the process of synthesizing a heavy element, the kinetic energy of projectile transfers the whole energy to the target and converted it into the excitation energy of the compound nucleus. In other words, it can be said that, the total transfer of kinetic energy, angular momentum and mass of projectile to the target takes the composite system to the higher level from the ground state. At the excited states, the compound system possessed with large amount of energy and momenta is hot enough and ready to decay the ground state due to its instability. The excitation energy of CN can be determined by the Q-value and kinetic energy of the nuclear fusion reaction. The time period of CN staying at the excited state lies typically in the range of 10^{-19} to 10^{-15} seconds which is considered relatively larger than the time of transition of an incident particle across the target ($\sim 10^{-22}$ seconds). That is why, the formation of a compound system is considered as a relatively long lived system and also an intermediate state of the projectile-target combination. One more thing can be added here that, after decay of CN from the excited state to the ground state, the reversible process is not possible or one can say that the composite system loses its memory of formation process. The nuclear fusion-fission reaction can be expressed as a two-stage process, as follows:

- Initially, the projectile hits the target and form a compound nucleus ($a+A \rightarrow Y^*$).
- Secondly, the compound nucleus in the excited state decays to the ground state with the emission of either a gamma radiation or fragments ($Y^* \rightarrow \gamma + Y$ or $Y^* \rightarrow b + B$).

In the present work, the nuclear fusion reactions occurred by heavy-ion collisions at the low energy region (<15MeV/nucleon) are considered to examine the interaction behavior between the colliding nuclei.

During the heavy-ion collision in nuclear fusion reaction, there is a formation of interaction potential between two nuclei. A built of interaction potential is generally due to Coulomb repulsion between the positively charged nucleons (protons), the rotation of nuclei and an attractive short-ranged nuclear/strong interaction between the colliding nuclei. In other words, one can simply define the total interaction potential between two colliding nuclei as a sum of Coulomb potential, centrifugal potential and nuclear potential. Basically, to study the nuclear properties, the ion-ion interaction potential is a very important and helpful tool to illustrate the behavior of nuclear fusion interactions.

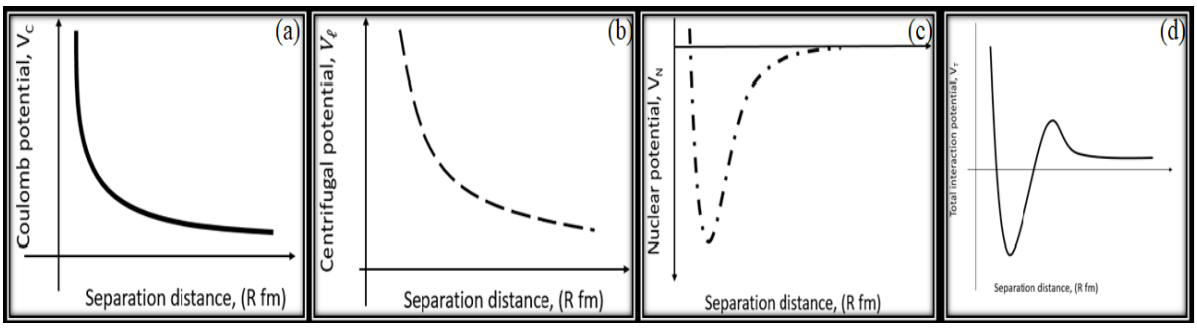

Fig. 1.3 Schematic diagrams of (a) Coulomb potential V_C, (b) centrifugal potential V_ℓ, (c) nuclear potential V_N and (d) total interaction potential V_T as a function of separation distance R (fm).

1.4 Ion-ion interaction potential:

At the level of nucleus-nucleus interaction, the repulsive Coulomb potential as a single term is not sufficient enough to illustrate the nuclear interactions. So, a proper and better understanding regarding the ion-ion collisions can be built by adding an appropriate knowledge of nuclear potential with a well-defined Coulomb potential. It has been said from the earlier observations that, experimentalists are not able to detect the fusion barriers formed due to composition of repulsive and attractive potentials in between two nuclei. Thus,

so many theoreticians have given various theoretical models which help to extract the knowledge of fusion barriers [6-8].

1.5 Proximity potential:

Generally, in these models, a simple analytical formulation is used to calculate the nucleus-nucleus interaction potential which is named as nuclear proximity potential. All of the proximity potentials from different models are developed on the basis of proximity theorem [9]. According to this theorem, the nuclear potential is directly proportional to the mean curvature and the universal function terms. The first proportional term is dependent on the nuclear shape/radius, and the second one is just a function of separation distance between two curved surfaces of colliding nuclei.

Number of researchers have worked on the proximity theorem and made so many modifications and improvements in the nuclear radii or the universal functions, in order to justify the experimental data of a large variety of nuclear reactions. In literature [6-8], the role of different versions of proximity potentials has been explored by addressing either the empirical data or the fusion cross-sections, especially at the below barrier energies. In the following, a brief detail of few nuclear proximity potentials has been provided.

1. Proximity 1977 (Prox77) – J. Blocki, J. Randrup, W. J. Swiatecki, and C. F. Tsang were the researchers [9] who developed the original model of proximity potential.
2. Proximity 1988 (Prox88)- The improved model of proximity potential was introduced by the two scientists Moller and Nix [10].
3. Proximity 2000 (Prox00) – Two scientists named Mayers and Swiaecki reformed the proximity potential and called it as 2000 [11].
4. Modified Proximity 2000 (Prox00 DP) – Royer and Rousseau [12] were the two scientists who gave another improved form of proximity potential.
5. Bass 1973 (Bass 73) – This potential [13] was introduced in 1973 on the basis of liquid drop model.
6. Bass 1977 (Bass 77) – On the basis of liquid drop model, another modified form of Bass 77 [14] results in nucleon-nucleon potential in 1977.

7. Bass 1980 (Bass 80) – Bass again improved the proximity potential in 1980 and called it as Bass80 [15].
8. Christensen and Winther 1976 (CW 76) – This model [16] was based on the heavy ion elastic scattering data.
9. Broglia and Winther 1991 (BW 91) – This model is advanced form of proximity potential given by Broglia and Winther in 1991 [15].
10. Aage winther (AW 95) – This model was introduced by Aage winther [17] in 1995 where the previous potential parameter was adjusted for heavy ion elastic scattering.
11. Ngô 1980 (Ngô 80) – H. Nĝo and Ch. Nĝo [18] gave this proximity potential.
12. New Denisov Potential (Denisov DP) - This model of proximity potential was given by Denisov [19].

In literature [9-19], the relevance of above mentioned proximity potentials has been observed in addressing the properties of nuclear fusion reactions. The radius as well as the surface energy coefficient terms involved in the proximity potentials are found to be dependent on the asymmetry parameter (A_s=|N-Z|/(N+Z), here N and Z are neutron and proton number of composite system). In view of this, the variations of different nuclear radii used within the above mentioned proximity potentials have been analyzed with respect to the asymmetry parameter [20,21]. The radii used in different proximities are also swapped within the proximity potentials in order to check the effect of radii on fusion barriers characteristics. It has been concluded from the analysis that, due to the change in nuclear radius, the fusion barrier height of the interaction changes, which in turn, shows respective variations in the calculation of fusion cross-sections.

In the present work, we have adopted few proximity potentials, like Prox77, Prox00 and Denisov DP. It has been observed that, the nuclear radii of later two proximity potentials are showing variations in the barrier heights (V_B) and barrier position (R_B) [21]. In view this, the intention of present work is to use the radii of Prox00 and Denisov DP within the proximity potential of Prox77, in order to analyze the respective variations in the fusion barrier height and position of the potential. For the calculation of fusion cross-sections, the Wong formula [22] has been taken into account. A comprehensive description regarding the formula is provided in the following section.

1.6 Wong formula:

In the nuclear fusion reactions, it is very important and an interesting aspect to measure the fusion barrier height between the colliding nuclei. Such measurement provides the knowledge of nuclear fusion process. The projectile with sufficient energy has to pass through the fusion barrier to fuse into the target. Therefore, the probability of penetration through the barrier illustrates the fusion probability of the two colliding nuclei. In view of this, a simple analytical expression obtained from the ingoing-wave strong-absorption model is used to calculate the fusion probability. Wong has established a formula [22] to calculate the fusion cross-sections on the basis of above mentioned absorption model, which is named after his name, that is Wong formula [21]. The details are given in Chapter 2.

In Wong formula, the theoretically calculated fusion barrier height (V_B), barrier position (R_B) and barrier curvature ($\hbar\omega_B$) as input values are introduced within the formula. For a particular nuclear fusion reaction, if the experimental data is available for the reaction then, one can calculate the fusion cross-sections at each and every values of incident energies ($E_{c.m.}$) provided in the data. In addition to this, it has been analyzed from the previous work [21] that, with the use of various versions of proximity potentials within the Wong model, the fusion cross-section changes due to change in barrier characteristics.

In view of above, the present work has been worked out to observe the variations in Prox77 in the calculation of fusion cross-sections for ^{16}O, ^{40}Ca and ^{48}Ca-induced reactions, via using the nuclear radii of Prox00 and Denisov DP within Prox77 proximity potential.

1.7 Proposed Work:

As it is mentioned in the above sections that, the fusion barrier height of the total interaction potential gets influenced with the change in nuclear radius. Thus, in the present work, the variations in the barrier height of Prox77 proximity

potential has been observed by using the nuclear radii of Prox00 and Denisov DP within the Prox77. The respective changes in the fusion barrier heights have been further analyzed in the calculation of fusion cross-sections using Wong formula. The theoretically calculated fusion cross-sections for ^{16}O, ^{40}Ca and ^{48}Ca-induced reactions are compared with the corresponding experimental data [23-27].

Chapter 2

Proximity potential and Wong formula

Chapter 2

Methodology

2.1 Total interaction potential:

At the level of nucleus-nucleus interaction, the repulsive potentials that is, Coulomb potential ($V_{Coul.}$) and centrifugal potential ($V_{Ang.}$) are not sufficient enough to illustrate the nuclear interaction. So, a proper understanding regarding the ion-ion potential can be built by adding an appropriate knowledge of nuclear potential with the well-defined $V_{Coul.}$ and $V_{Ang.}$ potentials.

$$\boldsymbol{V_{Tot.}(R) = V_{Coul.}(R) + V_{Prox.}(R) + V_{Ang.}(R).} \quad \textbf{(1)}$$

Here, the total interaction potential $V_{Tot}(R)$ is a function of the separation distance 'R' between two interacting nuclei. The detail of each term of $V_{Tot.}(R)$ are explained in the following sections.

The repulsion potential due to positively charged nucleus is defined as the long-range coulomb potential, which is expressed as follows for spherical nuclei.

$$\boldsymbol{V_{Coul.}(R) = \frac{Z_{Proj,}Z_{Tar.}e^2}{R}.} \quad \textbf{(2)}$$

The rotational energy of the composite system due to angular momentum is defined as

$$\boldsymbol{V_{Ang.}(R) = \frac{\hbar^2 \ell(\ell+1)}{2I_{N.S.}}.} \quad \textbf{(3)}$$

Here, ℓ is the quantum number of angular momentum. $I_{N.S.}$ is the moment of inertia for the case of non-sticky target and projectile.

The Coulomb interaction potential and the centrifugal potential are the two well-defined potentials. However, because of impulsive nature of various interacting nuclei, the nuclear interaction potential is not well-defined. Various nuclear proximity potentials are available in literatures. A few choices of proximity

potentials are discussed in the following sections, which are used in present work.

2.2 Proximity 1977 (Prox77):

As discussed in Chapter 1 that the nuclear proximity potential works within a very short-range of separation distance (~ 2 fm). To define the nucleus-nucleus potential within this proximity region, J. Blocki et al. [9] has developed a very simple analytical expression on the basis of Proximity theorem and termed it as the proximity potential $V_{Prox.}(R)$.

The nuclear proximity potential (Prox77) derived by J. Blocki et al [9] is given as

$$\boldsymbol{V_{Prox.}(R) = 4\pi\gamma b\bar{R}\Phi(s).} \quad \textbf{(4)}$$

Here, γ is the surface coefficient term, 'b' is the surface diffuseness term, $\bar{R}$ is the mean curvature radius and Φ (s) is the universal function. The universal function is independent of the nuclear shape and structure, but function of 's' (minimum distance between two curved spherical surfaces of two nuclei).

The mean curvature radius '$\overline{\mathrm{R}}$' is given as follows

$$\boldsymbol{\overline{R} = \frac{C_{Proj.}C_{Targ.}}{C_{Proj.}+C_{Targ.}}.} \quad \textbf{(5)}$$

Here,

$$\boldsymbol{C_i = R_i\left[1 - \left(\frac{b}{R_i}\right)^2 + \cdots\right],} \quad \textbf{(6)}$$

where, i = Proj., Targ. stands for projectile and target, respectively.

The effective sharp radius R_i term in the above Eq.(6) is written as follows

$$\boldsymbol{R_i = 1.28A_i^{1/3} - 0.76 + 0.8A_i^{-\frac{1}{3}} fm.} \quad \textbf{(7)}$$

In Eq.(4), the universal function $\Phi(s)$ for Prox77 is expressed as follows

$$\boldsymbol{\Phi(s) = \begin{cases} -\frac{1}{2}\,(s-2.54)^2 - 0.0852(s-2.54)^2, s \le 1.2511 \\ -3.437e^{\left(\frac{-s}{0.75}\right)}, s \ge 1.2511 \end{cases}} \quad \textbf{(8)}$$

In Prox77, both of the factors $\Phi(s)$ and $\bar{R}$ term do not depend on the isospin content. On the other hand, in Eq.(4) , the surface energy coefficient 'γ' term is dependent on isospin term i.e. the ratio of number of neutron (N) and number of proton (Z).

$$\boldsymbol{\gamma = \gamma_0 \left[1 - k_s \left(\frac{N-Z}{A}\right)^2\right].} \quad \textbf{(9)}$$

In the above equation, γ_0 and k_s are the constant values i.e. $\gamma_0 = 0.9517\ MeV/fm^2$ and $k_s = 1.7826$.

For the case of symmetric colliding pair, the number of neutrons is equal to the number of proton (N=Z). Thus, the surface energy coefficient 'γ' term is given as

$$\boldsymbol{\gamma = \gamma_0 = 0.9517 \frac{MeV}{fm^2}.} \quad \textbf{(10)}$$

In addition to the above, the value of 'γ' reduces to $0.5276\ MeV/fm^2$, if the ratio $\frac{N-Z}{N+Z}$ in Eq. (9) becomes half.

2.3 Proximity 2000 (Prox00):

Proximity 2000 or Prox00 is defined as the modified version of Eq. (4), given by Myers and Swaitecki [11]. With an adequate knowledge of nuclear radii and surface coefficient terms, the proximity potential of Eq. (4) is modified by using the concept of droplet model [28,29]. In view of this, the matter radius (C_i) is expressed as follows:

$$\boldsymbol{C_i = c_i + \frac{N_i}{A_i} t_i, (i = 1, 2).} \quad \textbf{(11)}$$

Here, 'c_i' represents the half-density radii of the nuclear charge distribution and 't_i' is defined as the neutron skin of the nucleus. The value of 'c_i' is calculated by following the detail given in [30,31] and also provided below.

$$\boldsymbol{c_i = R_{00i}\left(1 - \frac{7}{2}\frac{b^2}{R_{00i}^2} - \frac{49}{8}\frac{b^4}{R_{00i}^4} + ..\right).} \quad \textbf{(12)}$$

Here,

$$\boldsymbol{R_{00i} = \sqrt{\frac{5}{3}\langle r^2\rangle^{\frac{1}{2}}}.}$$

The $\langle r^2\rangle$ in the above equation is the mean-square value of nuclear charge radius. The above equation is valid for even-even nuclei which lies in the range of $8 \leq Z \leq 38$ only. for the case $Z \leq 38$, R_{00i} is given as follows:

$$\boldsymbol{R_{00i} = 1.240A_i^{1/3}\left\{1 + \frac{1.646}{A_i} - 0.191\left(\frac{A_i - 2Z_i}{A_i}\right)\right\} fm,} \quad \textbf{(13a)}$$

$$\boldsymbol{R_{00i} = 1.256A_i^{1/3}\left\{1 - 0.202\left(\frac{A_i - 2Z_i}{A_i}\right)\right\} fm.} \quad \textbf{(13b)}$$

Further, the second factor that is, neutron skin 't_i' is given in Eq. (11) is also calculated using the droplet model as follows:

$$\boldsymbol{t_i = \frac{3}{2}r_0\left(\frac{JI_i - \frac{1}{12}c_iZ_iA_i^{-1/3}}{Q + \frac{9}{4}JA_i^{-1/3}}\right).} \quad \textbf{(14)}$$

Here, the value of r_0 is 1.14 fm, 'J', which is named as symmetric energy coefficient, has value 32.65 MeV, and $c_i\left(=\frac{3\,e^2}{5r_0}\right) = 0.757895\ MeV$. The value of neutron skin stiffness coefficient 'Q' is 35.4 MeV. Also, the term 'γ' of Prox00 is given as follows :

$$\boldsymbol{\gamma = \frac{1}{4\pi r_0^2}\left[18.63 - Q\frac{\left(t_1^2 + t_2^2\right)}{2r_0^2}\right].} \quad \textbf{(15)}$$

Here, 't_1' and 't_2' are calculated from Eq. (14).

Now, the universal equation $\Phi(s)$ of the Prox00 is given as:

$$\Phi(s) = \begin{cases} -0.1353 + \sum_{n=0}^{5} \left[\frac{c_n}{(n+1)}\right](2.5 - s)^{n+1}, 0 < s \leq 2.5 \\ -0.09551 exp\left[\frac{(2.75-s)}{0.7176}\right], s \geq 2.5 \end{cases} . \quad (16)$$

The values of different constant c_n for n = 0,1,2,3,4,5 are -0.1886, -0.2628, -0.04562, 0.069136 and -0.011454, respectively. The exponential expression is the for s ≥ 2.5 of the extended Thomas-fermi approach of the proximity potential. This potential is termed as Prox00.

2.4 New Denisov DP (Denisov DP):

The new Denisov proximity potential which is generally represented as Denisov DP [19] is expressed as an analytically formulation of the proximity potential as give below:

A simple expression for the nuclear part of the interaction potential $V_{Prox.}(R)$ between the two spherical nuclei is given by:

$$V_{Prox.}(R) = -1.989843 \frac{R_{Proj.}R_{Targ.}}{R_{Proj.} + R_{Targ.}} . \Phi\big(r - R_{Proj.} - R_{Targ.} - 2.65\big) \times \left[1 + 0.003525139\left(\frac{A_1}{A_2} + \frac{A_2}{A_1}\right)^{\frac{3}{2}} - 0.4113263(I_1 + I_2)\right]. \quad (17)$$

Here, I_i is the ratio of (N_i-Z_i) and (N_i+Z_i) that is, $\left[\frac{N_i - Z_i}{N_i + Z_i}\right]$.

The effective nuclear radius R_i for Denisov DP potential is given as follows:

$$R_i = R_{ip}\left(1 - \frac{3.413817}{R_{ip}^2}\right) + 1.284589\left(I_i - \frac{0.4A_i}{A_i+200}\right). \quad (18)$$

Here, 'R_{ip}' is the radius of proton and is given by Eq. (13). Now, the universal function $\Phi(s = r - R_{Proj.} - R_{Targ.} - 2.65)$ of Denisov DP potential is a complex form and given as follows:

$$\Phi(s) = \begin{cases} 1 - \frac{s}{0.7881663} + 1.229218s^2 \\ -0.2234277s^3 - 0.1038769s^4 \\ -\frac{R_{Proj.}R_{Targ.}}{R_{Proj.}+R_{Targ.}}(0.1844935s^2 + 0.07570101s^3) \\ +(I_1+I_2)(0.04470645s^2 + 0.03346870s^3), \\ for -5.65 \le s \le 0 \\ \left[1 - s^2\left[0.05410106\frac{R_{Proj.}R_{Targ.}}{R_{Proj.}+R_{Targ.}}exp\left(-\frac{s}{1.760580}\right) \right.\right.\right. \\ \left.\left.\left. -0.53954420(I_1+I_2)exp\left(-\frac{s}{2.424408}\right)\right]\right] \\ \times exp\left(-\frac{s}{0.7881663}\right) \\ for\ s \ge 0 \end{cases}. \quad (19)$$

This above form of the universal function depends not only on the separation distance 's', but also depends on the mass number and the neutron excess content that is, I_i.

2.5 Wong formula:

According to Wong formula [22], the fusion cross section in terms of ℓ-partial waves for the two colliding nuclei is defined as a function of center of mass energy '$E_{c.m}$' and given as follows:

$$\sigma_{fus.}(E_{c.m}) = \frac{\pi}{k^2}\sum_{\ell=0}^{\ell_{max}}(2\ell+1)P_\ell\,(E_{c.m.}). \quad (20)$$

Here, $k = \sqrt{\frac{2\mu E}{\hbar^2}}$. $\mu = \frac{A_1 A_2}{A_1 A_2}$ is the reduced mass. 'P_ℓ' defines the transmission penetration probability to tunnel through the inverted harmonic oscillator of interaction potential (Eq.(1)), using the Hill-Wheeler approximation [32]. The barrier of interaction potential can be calculated from Eq. (1).

In Eq. (20), the term penetrability, P_ℓ in terms of the barrier height $V_B^\ell(E_{c.m})$ and the barrier curvature $\hbar\omega_B\ (E_{c.m})$ is given as follows

$$\boldsymbol{P_\ell = \left[1 + exp\left(\frac{2\pi(V_B^\ell(E_{c.m}) - E_{c.m.})}{\hbar\omega_B\ (E_{c.m})}\right)\right]^{-1}}. \qquad \textbf{(21)}$$

The barrier curvature $\hbar\omega_B$ is calculated by taking double differential of total potential $V_{Tot.}(R)$ as given below:

$$\hbar\boldsymbol{\omega_B(E_{c.m}) = \hbar\left[\left|\frac{d^2V_\ell(R)}{dR^2}\right|_{R=R_B^\ell} \Big/ \mu\right]^{1/2}}. \qquad \textbf{(22)}$$

Also, Wong considered two conditions as given below:

- $\hbar\boldsymbol{\omega_\ell \approx \hbar\omega_0}$, and
- $\boldsymbol{V_B^\ell \approx V_B^0 + \frac{\hbar^2\ell(\ell+1)}{2\mu {R_B^0}^2}}$.

Here, the fusion barrier height 'V_B^0' is calculated by taking ℓ=0 in Eq. (1). Thus,

$$\boldsymbol{V_B^0 = V_{Prox.}(R = R_B^0) + V_{Coul.}(R = R_B^0)}. \qquad \textbf{(23)}$$

Eq. (20) is carried out by taking the ℓ-summation and given as follows:

$$\boldsymbol{\sigma_{fus.}(E_{cm}) = \frac{{R_B^0}^2\hbar\omega_0}{2E_{c.m.}} \ln\left[1 + \exp\left\{\frac{2\pi}{\hbar\omega_0}\left(E_{c.m.} - V_B^0\right)\right\}\right]}. \qquad \textbf{(24)}$$

Chapter 3

Outcomes and Discussions

Chapter 3

Fusion cross-sections using different nuclear proximity potentials and radii at low energy

As discussed in Chapter1 that, a variety of nuclear proximity potentials are utilized for investigating and exploring the nuclear properties via addressing the behavior of nuclear fusion reactions at the below as well as above barrier energies [20,21]. In Ref. [21], different forms of nuclear proximity potentials are considered for explaining the fusion-evaporation cross-sections of Ni-based reactions. In the results, Prox77 and Prox00 are found to show fusion hindrance, at the below-barrier energies, for heavy-mass region with the use of Wong formula [22]. On the basis of this observation, an attempt has been done in the present work by considering the nuclear radii of Prox00 and Denisov DP potentials within the formalism of Prox77, in order to explore the respective variations on the fusion barrier characteristics (barrier height V_B and barrier position R_B) and subsequently on the fusion cross-sections for the nuclei of intermediate and heavy-mass regions.

Here, in the present work, the effect of Prox77 has been investigated for the isotopes of Zr* and Nd* compound nuclei formed from $^{16}O+^{74}Ge$, $^{40}Ca+^{40}Ca$, $^{48}Ca+^{48}Ca$, $^{40}Ca+^{90}Zr$, $^{40}Ca+^{96}Zr$ and $^{48}Ca+^{96}Zr$ reactions in terms of fusion cross-sections. The analysis is also exercised for nuclear radii of Prox00 and Denisov DP potentials introduced within the Prox77 potential. The results obtained are compared with the experimental data [23-27] of the above mentioned fusion reactions.

3.1 Observations and discussion:

Here, we have considered different choices of proximity potentials i.e. Prox77, Prox00 and Denisov DP. The total interaction potential $V_{Tot.}(R)$ has been plotted using the above given proximity potentials. Also, the nuclear radii of Prox00 and Denisov DP are introduced within the Prox77 potential and corresponding variation on total interaction potential has been observed. In Fig.3.1, a comparison of Prox77, Prox00 and Denisov DP has been depicted using (a) standard universal functions (see Eqs. (8), (16) and (19)) and (b) different radii of Prox00 and Denisov DP (see Eqs. (13) and (18), respectively) within Prox77 for $^{40}Ca+^{40}Ca$ reaction. The standard universal function means that respective

universal function of Prox77, Prox00 and Denisov DP are used along with their radii. From panel (a) of Fig.3.1, it is observed that, the barrier height (V_B) of Denisov DP potential is the highest one followed by that of Prox77 and Prox00 potentials. On the other hand, in panel (b) of Fig.3.1, by using nuclear radii of Prox00 and Denisov DP within Prox77, V_B of Denisov DP gets reduced by 3 MeV and V_B of Prox00 gets down by 1 MeV.

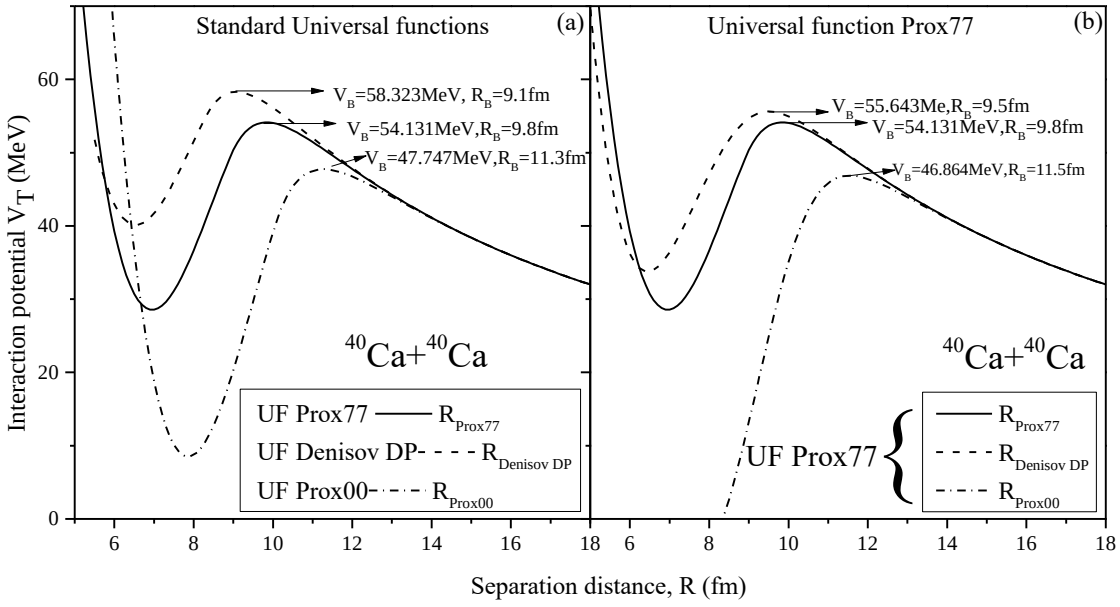

Figure 3.1: Comparison of Prox77, Prox00 and Denisov DP using (a) Standard universal function and (b) different radii within Prox77 in terms of total interaction potential $V_{Tot.}(R)$ for ^{40}Ca +^{40}Ca reaction.

From above analysis, it can be said clearly that the nuclear radii of Prox00 and Denisov DP as the input within the Prox77 potential gives deeper pocket and lower barrier height. In general, it can be said that due to change in nuclear radius within the Prox77 potential, the fusion barrier height gets influenced.

Further, the role of different choices of nuclear radii has been observed for Zr^* isotopes, as shown in Fig.3.2. From this figure, all the radii changes linearly and the nuclear radius of Prox00 is larger than that of Prox77 and Denisov DP. As a consequence, the larger nuclear radii gives lower barrier height.

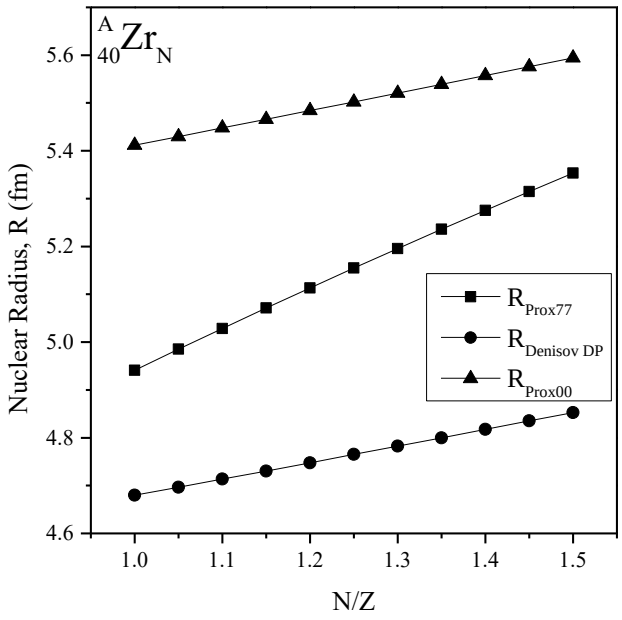

Figure 3.2: Variation of the different choices of nuclear radii for Zr^{*} isotopes.

It is known that, larger value of nuclear radius gives larger value of fusion cross-sections (see Eq. (24)). In view of this, a comparison of different radii within the Prox77 potential has been analyzed in terms of the total interaction potential and fusion cross-section for Zr^{*} isotopes. The compound nuclei $^{80,90,96}Zr^{*}$ are formed from ^{16}O,^{40}Ca and ^{48}Ca-induced reactions [23-27].

As discussed in Fig 3.1, the barrier height of Denisov DP is the largest followed by Prox77 and Prox00 for ^{40}Ca +^{40}Ca reaction. The result is consistent for ^{16}O+^{74}Ge and ^{48}Ca +^{48}Ca reactions as well as it is clear from Fig.3.3. On the other hand, the influence of different barrier heights and positions has been observed in the calculation of fusion cross-section. Further, the theoretically estimated fusion cross-sections are compared with the experimental data of above mentioned ^{16}O,^{40}Ca and ^{48}Ca-induced reactions. It has been observed from panel (d) of Fig.3.3 that, due to the lowest barrier height of Prox00, the calculated fusion cross-sections overestimate the data of ^{40}Ca +^{40}Ca reaction.

However, the highest barrier height of Denisov DP hinders the fusion cross-sections at the below barrier energies. Here, Prox77 addresses the fusion data very nicely across the Coulomb barrier with the use of Wong formula.

Now, with the increase in number of neutrons of Zr^*, the result obtained using radii of Prox00 and Denisov DP is consistent for $^{90,96}Zr^*$ compound nucleus. However, Prox77 overestimates the data with a very small amount. A detail of calculated fusion cross-sections is provided in Tables 1-3 for the above mentioned reactions.

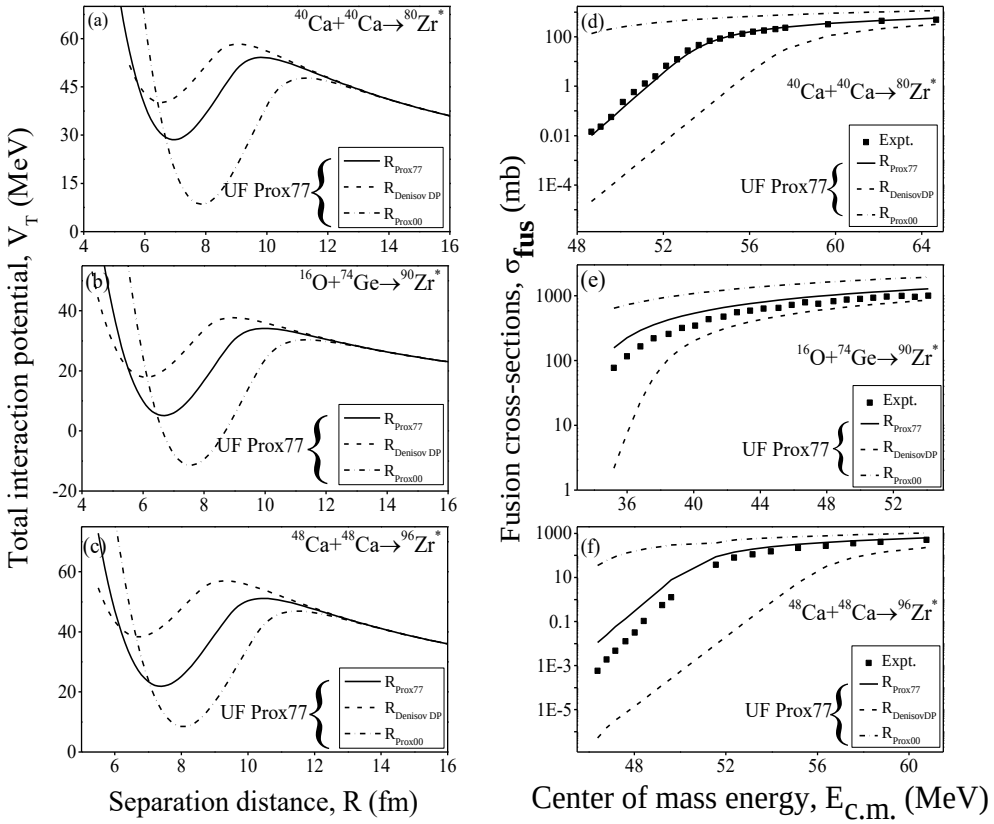

Figure 3.3: (a), (b) and (c) shows the comparison of total interaction potential $V_{Tot.}(MeV)$ and (d), (e) and (f) gives the fusion cross-section $\sigma_{fus.}(mb)$ using different choices of nuclear radii for $^{80,90,96}Zr^*$.

Further, the above analysis is extended for heavy-mass region. Now, the role of different radii from Prox00 and Denisov DP has been explored in reference to Prox77 for the formation of Nd^* isotopes formed from ^{40}Ca and ^{48}Ca-induced reactions.

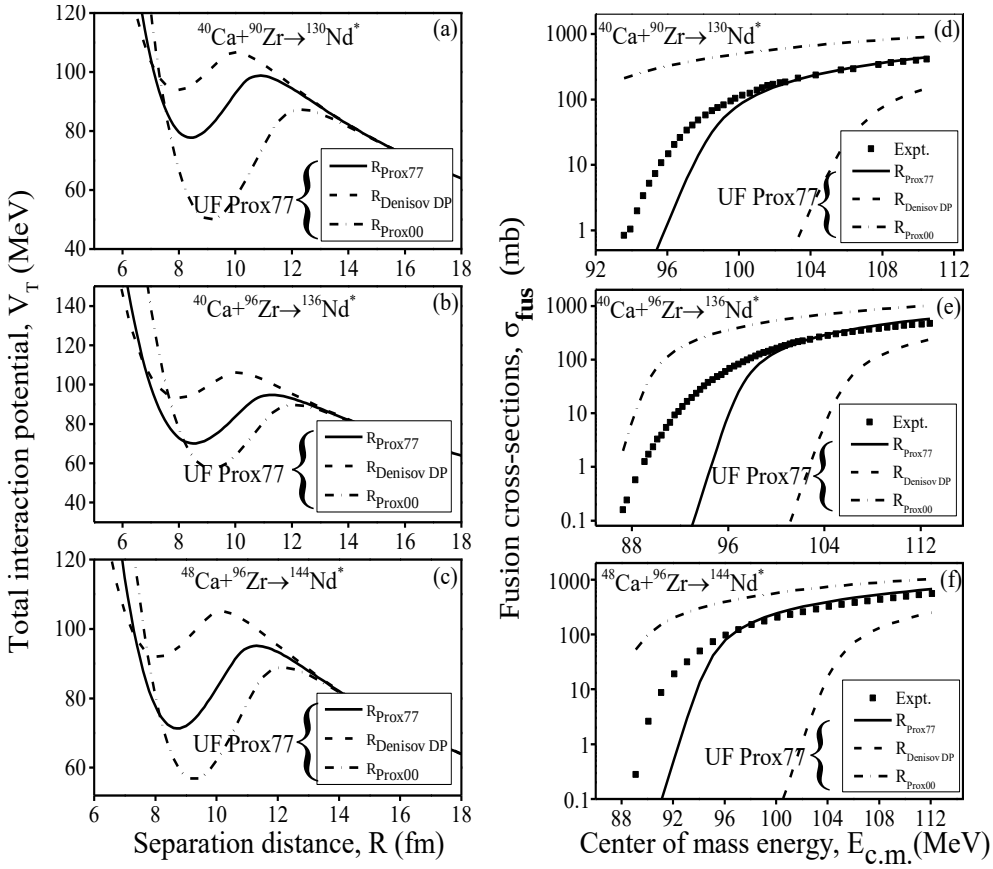

Figure 3.4: Same as Fig. 3.3, but for $^{40}Ca+^{90,96}Zr$ and $^{48}Ca+^{96}Zr$ reactions [23-27].

In Fig. 3.4, comparison of different nuclear radii has been observed in terms of total interaction potential and fusion cross-sections. For the case of heavy-mass region, the pockets of Denisov DP and Prox77 are very much shallower than Prox00. As a consequence, in the calculation of fusion cross-sections, the results obtained using Prox77 and Denisov DP show the fusion hindrance. However, Prox00 overestimates the experimental data of $^{40}Ca+^{90}Zr$, $^{40}Ca+^{96}Zr$ and $^{48}Ca+^{96}Zr$ reactions. The overestimation of calculated fusion cross-section, due to Prox00 can be handled using extended ℓ-summed Wong model [21], which is not done in the present work.

Table 1: The fusion cross-section for $^{40}Ca+^{40}Ca$ [24], calculated by Wong formula.

$E_{c.m.}$(MeV)	Temperature (T)	Fusion cross-section,$\sigma_{fus.}$(mb)			
		Expt.	Prox77	Denisov DP	Prox00
48.66	2.027	0.01434	0.0102	2.16E-05	135.08
49.09	2.039	0.02282	0.02156	4.28E-05	169.5
49.58	2.053	0.05587	0.0501	9.54E-05	207.92
50.12	2.068	0.2295	0.132	2.34E-04	251.36
50.63	2.082	0.5716	0.326	5.47E-04	291.94
51.14	2.096	1.262	0.789	0.00125	330.81
51.63	2.11	2.469	1.84	0.00282	367.55
52.14	2.124	6.704	4.46	0.00657	405.03
52.65	2.137	12.03	10.02	0.01509	441.8
53.14	2.151	27.5	20.21	0.03325	475.85
53.65	2.164	46.07	37.02	0.0763	512.96
54.16	2.178	67.23	59.54	0.1766	547.73
54.64	2.191	84.02	83.85	0.3831	580
55.15	2.204	116.4	111.93	0.895	613.56
55.68	2.218	131.2	140.86	2.0959	647.89
56.17	2.231	161.1	167.41	4.4727	680.09
56.68	2.244	178.4	194.78	9.2853	711.97
57.21	2.257	201	222.77	18.72	744.54
57.67	2.269	230.4	247.71	31.02	772.39
59.65	2.319	318	346.48	110.67	888.33
62.14	2.38	438.1	463.16	216.67	1023.98
64.67	2.44	490.8	572.97	316.05	1151.47

Table 2: Same as Table 1, but for $^{16}O+^{74}Ge$ reaction [23].

$E_{c.m.}$(MeV)	Temperature (T)	Fusion cross-section,$\sigma_{fus.}$(mb)			
		Expt.	Prox77	Denisov DP	Prox00
35.2	2.191	76.7	157.04	2.18	644.15
36	2.21	116	225.47	7.59	724.98
36.8	2.228	164.5	292.65	23.25	802.29
37.6	2.246	220	356.99	55.38	876.84
38.5	2.267	256.3	426.82	106.6	956.66
39.3	2.285	317.1	485.88	156.91	1025.15
40.1	2.303	346	542.63	206.58	1091.1
40.9	2.32	434	597.76	254.78	1153.89

41.8	2.34	473	657.29	307.54	1221.77
42.6	2.357	553	707.69	352.61	1280.25
43.4	2.375	589	757.28	395.76	1336.86
44.2	2.392	631	803.7	437.37	1390.89
45.1	2.411	649	854.64	482.41	1449.39
45.9	2.428	722	898.26	521.51	1500.13
46.7	2.445	788	941.48	558.87	1548.67
47.5	2.461	754	982.32	595.48	1596.19
48.4	2.48	821	1026.55	634.79	1647.73
49.2	2.496	868	1064.6	669.1	1691.38
50	2.513	890	1102.23	701.83	1734.01
50.8	2.529	932	1137.98	733.42	1775.98
51.6	2.545	965	1172.79	764.23	1816.74
52.5	2.563	989	1211.75	798.14	1860.31
53.3	2.579	964	1244.75	827.53	1898.83
54.1	2.594	1000	1276.2	855.49	1935.25

Table 3: Same as Table 1 and 2, but for ^{48}Ca+^{48}Ca reaction [25].

$E_{c.m}$(MeV)	Temperature (T)	Fusion cross-section,$\sigma_{fus.}$(mb)			
		Expt.	Prox77	Denisov DP	Prox00
46.39	2.064	5.80E-04	0.01123	5.18E-07	34.99
46.79	2.073	0.00188	0.0249	1.55E-06	59.43
47.17	2.082	0.00473	0.0587	3.36E-06	89.01
47.61	2.092	0.0126	0.133	7.04E-06	123.87
48.02	2.102	0.03181	0.305	1.45E-05	159.52
48.41	2.11	0.1045	0.667	2.92E-05	192.81
49.22	2.129	0.5597	3.34	1.31E-04	260.8
49.61	2.138	1.249	7.76	2.62E-04	297.72
51.56	2.181	37.525	88.15	0.00925	371.12
52.36	2.198	78.905	139.85	0.0392	506.9
53.17	2.216	111.36	192.45	0.1711	565.56
53.97	2.233	152.74	243.15	0.723	621.82
55.16	2.259	220.08	316.94	5.79	703.7
56.37	2.284	270.06	386.83	31.85	782.3
57.57	2.309	354.77	455.58	82.11	857.24
58.76	2.334	409.13	518.79	136.58	929.68
60.77	2.374	504.87	624.04	228.8	1043.98

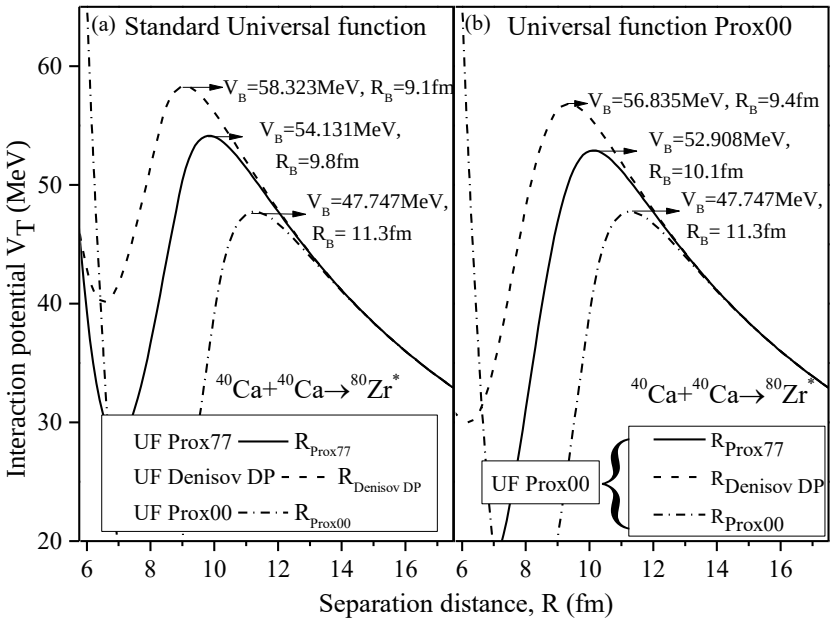

Fig 3.5 The total interaction potential for $^{40}Ca+^{40}Ca$ using standard and Prox00 universal function within different interaction potential.

Further, a test calculation has been done by considering the nuclear potential of Prox00 as shown in Fig. 3.5. The nuclear radii of Prox77 and Denisov DP are used within Prox00 to observe the respective variations in the barrier height V_B and barrier position R_B. The results obtained are similar to that of Fig. 3.1 for the case of $^{40}Ca+^{40}Ca$.

3.2 Conclusions:

From the above results and discussions, it has been concluded that, the different nuclear radii referred from Prox00 and Denisov DP potentials within the Prox77 potentials lower (enlarge) the fusion barrier height V_B (barrier position R_B) of the interaction potential. For the formation of $^{80,90,96}Zr^*$ [23-25] isotopes, it has been observed that Prox77 gives better results for explaining the fusion cross-sections using Wong formula as compared to Prox00 and Denisov DP. On the other hand, for the case of heavy-mass region that is $^{130,136,144}Nd^*$ [26-27], the shallower pockets of Prox77 and Denisov DP hinder the data at below barrier energies. However, Prox00 overestimates the data. It is also concluded that for reactions showing the fusion hindrance one can use radius of Prox00 within the universal function of Prox77 which in turns leads to the lowering of barrier and

increase in the fusion cross-section. Thus, change in the radius might help in dealing with fusion hindrance in some reactions below the Coulomb Barrier energies. This result needs further investigations for the different combination of target and projectile around the Coulomb barrier.

Summary

In the present work, different nuclear radii taken from Prox00 and Denisov DP proximity potentials are used within the Prox77 to analyze the respective variations on the total interaction potential and the fusion cross-sections. The barrier height gets reduced by 3 MeV due to the nuclear radius of Denisov DP and by 1 MeV with the use of Prox00 for $^{40}Ca+^{40}Ca \rightarrow ^{80}Zr^{*}$ reaction. Further, the analysis is extended for other isotopes of Zr, i.e. $^{90,96}Zr^{*}$, and Nd^{*} ($^{130,136,144}Nd^{*}$) in terms of interaction potential and fusion cross-section calculated using the Wong formula. The results obtained using Wong formula for the formation of intermediate and heavy-mass regions ($^{80,90,96}Zr^{*}$ and $^{130,136,144}Nd^{*}$) are compared with the experimental data across the Coulomb barrier. The calculated fusion cross-sections overestimate the data due to larger nuclear radius of Prox00 and hinders the data due to smaller radius of Denisov DP. On the other hand, Prox77 has been found to perform better to address the data of $^{80,90,96}Zr^{*}$ isotopes across the Coulomb barrier. For the case of heavier mass-region $^{130,136,144}Nd^{*}$, Prox77 and Denisov DP give shallower pocket and larger barrier height as compared to Prox00 and hence show fusion hindrance, at the below barrier region. However, due to the lowest barrier height of Prox00, the corresponding potential overestimates the data which can be tackled with the use of extended l-summed Wong model (which is not done in the present work).

Future scope

In the future scope, the overestimation of fusion cross-section due to the largest nuclear radius of Prox00, which in turn gives the lowest barrier height, can be reduced in order to fit the experimental data, with the use of extended ℓ-summed Wong model. In addition to this, one can use different nuclear radii within the respective universal function of variety of nuclear potentials to analyze the variations on the interaction potential and fusion cross-sections for different target-projectile combinations from different mass-regions of periodic table at below as well as above the Coulomb barrier energies. Further, it is of interest to investigate role of radius in handling fusion hindrance phenomenon's at below barrier energies. Also, the above said results can be tested for variety of nuclear reactions along with the effect of deformations and orientations.

Reference:

[1] N. Wang, et al., Phys. Rev. C **74**, 044604 (2006).

[2] V. Y. Denisov, Phys. Lett. B **526**, 315 (2002).

[3] R. Bass, Nucl. Phys. A **231**, 45 (1974).

[4] R. Bass, Nuclear Reactions with Heavy Ions (Springer-Verleg, Berlin, 1980).

[5] J. Blocki, et al., Phys. (N.Y.) **105**, 427 (1977).

[6] J. Randrup and J. S. Vaagen, Phys. Lett. B **77**, 170 (1978).

[7] J. R. Birkelund and J. R. Huizenga, Phys. Rev. C **17**, 126 (1978).

[8] I. Dutt, and R. K. Puri, Phys. Rev. C **81**, 064609 (2010); ibid 81, 064608 (2010).

[9] J. Blocki, et al., Ann. Phys. (NY) **105**,427 (1977).

[10] P. Möller and J. R. Nix, Nucl. Phys. A **361**, 117 (1981).

[11] W. D. Myers and W. J. Swiatecki, Phys. Rev. C **62**, 044610 (2000).

[12] G. Royer and R. Rousseau, Eur. Phys. J. A **42**, 541 (2009).

[13] R. Bass, Phys. Lett. B 47, 139 (1973); Nucl. Phys. A **231**, 45 (1974).

[14] R. Bass, Phys. Rev. Lett. **39**, 265 (1977).

[15] W. Reisdorf, J. Phys. G: Nucl. Part. Phys. **20**, 1297 (1994).

[16] P. R. Christensen and A. Winther, Phys. Lett. B **65**, 19 (1976).

[17] A. Winther, Nucl. Phys. A **594**, 203 (1995)

[18] H. Nĝo and C. Nĝo, Nucl. Phys. A **348**,140 (1980)

[19] V. Y. Denisov, Phys. Lett. B **526**, 315 (2002).

[20] I. Dutt and R. K. Puri, Phys. Rev. C **81**, 064609 (2010).

[21] R. Kumar, Phys. Rev. C **84**, 044613 (2011).

[22] C. Y. Wong, Phys. Rev. Lett. **31**, 12 (1973).

[23] E. F. Aguilera, et al., Phys. Rev. C **52**, 3103 (1995).

[24] G. Montagnoli, et al., Phys. Rev. C **85**, 024607 (2012).

[25] G. Montagnoli, et al., Phys. Lett. B **679**, 95 (2009).

[26] H. Timmers, et al., Phys. Lett. **B 399,** 35 (1997).

[27] A. M. Stefanini, et al., Phys. Rev. **C 73**, 034607 (2006).

[28] W. D. Myers and W. J. Swiatecki, Ann. Phys. **55**, 395 (1969).

[29] W. D. Myers and W. J. Swiatecki, Nucl. Phys. A **336**, 267 (1980).

[30] C. W. de Jafer et. al., At Data Nucl. Data Tables **14**, 479 (1974).

[31] H. de Vries. et. al., At. Data Nucl. Data Tables **36**, 495-536 (1987).

[32] D. L. Hill and J. A. Wheeler, Phys. Rev. **89**, 1102 (1953).